High Temperatures-High Pressures, Vol. 50, pp. 167–184
Reprints available directly from the publisher
Photocopying permitted by license only
DOI: 10.32908/hthp.v50.1031

Contactless measurement of temperature-dependent viscosity and surface tension of liquid $Al_{69.1}Cu_{12.8}Ag_{18.1}$ eutectic alloy under microgravity conditions using the oscillating-drop-method

MITJA BECKERS*, MARC ENGELHARDT AND STEPHAN SCHNEIDER

[1]*Institut für Materialphysik im Weltraum, Deutsches Zentrum für Luft- und Raumfahrt (DLR), 51147, Cologne, Germany*

Thermophysical properties of the $Al_{69.1}Cu_{12.8}Ag_{18.1}$ eutectic liquid alloy are of particular interest for support of self-and inter-diffusion studies. In the presented work, $Al_{69.1}Cu_{12.8}Ag_{18.1}$-samples were processed contactlessly by electromagnetic levitation under microgravity conditions using the TEMPUS facility. The measurements were performed onboard the Airbus A310 Zero-G in parabolic flight campaigns. The oscillating-drop-method (ODM) was used for measurements of the viscosity via oscillations damping and surface tension via oscillations frequency. These were determined for temperatures in the range of 900–1500 K by analysis of the oscillation spectrum obtained from the electrical impedance. The latter was measured using the Sample Coupling Electronics. An Arrhenius-law $\eta(T) \propto \eta_\infty \exp(E_\eta / \mathrm{R}T)$ was used to fit the temperature-dependent viscosity data. The resulting fit parameters were $\eta_\infty = (0.632 \pm 0.160)$ mPas and activation energy of viscous flow $E_\eta = (2.344 \pm 0.233) \cdot 10^4$ J/mol. A linear law $\gamma(T) = \gamma_l + \gamma_T (T - T_m)$ was fit to the surface tension data yielding $\gamma_l = (0.9013 \pm 0.02625)\ \mathrm{Nm}^{-1}$ and $\gamma_T = -(0.7462 \pm 0.2675) \cdot 10^{-4}\ \mathrm{Nm}^{-1}\mathrm{K}^{-1}$. The Kozlov-model was applied to determine the enthalpy of mixing as $\Delta H_{mix} = -(18.576 \pm 0.018)$ kJ/mol.

Keywords: ODM, viscosity, ternary alloy, eutectic, AlCuAg, EML, TEMPUS, surface tension, Arrhenius, parabolic flight

*Corresponding author: mitja.beckers@dlr.de

1 INTRODUCTION

The modeling of thermophysical behavior of multi-component systems is an important step for understanding of fundamental physics and thus essential for predictivity of process parameters for industrial application. Calibration measurements of such systems, especially with "non-ideal" mixing behavior are vital for model validation. Brillo concluded that the ternary Al-Cu-Ag system has a strongly "non-ideal" mixing behavior, with $\Delta H_{mix} < 0$ and "excess"-viscosity $\eta^E > 0$ (Table 5.11) [1]. $Al_{69.1}Cu_{12.8}Ag_{18.1}$ has a low liquidus-temperature of $T_l = 774$ K [2] and is composed of well-studied binary systems. [2–5] High temperature soldering of Al with binary Ag-Cu is one of many practical applications of the system. [6] Another potential application is its usage as antimicrobial surface for spaceflight activities. [7] Thermophysical data, interface parameters and microstructural kinetics have been investigated systematically under normal gravity (1g) conditions for different compositions of the ternary alloy. [8–11] For fundamental research, self- and inter-diffusion-studies are carried out applying the shear-cell-method as described in [2]. Our measurements were performed to support those studies. Brillo *et al.* investigated the viscosities of various compositions of the ternary Al-Cu-Ag-system and observed viscosity changes by nearly an order of magnitude throughout the investigated concentration range. [11] Brillo *et al.* further summarized that no accepted expression exists for the concentration dependence of the viscosity although a number of different models have been suggested. [11] An overview of mostly phenomenological models for ternary and Al-based systems is given in [12–13]. The Kozlov-model [14] is derived strictly from physical principles. It relates the viscosities of pure elements to the enthalpy of mixing ΔH_{mix} of an alloy. All these findings emphasize the importance of measurements of viscosity and surface tension at the precise $Al_{69.1}Cu_{12.8}Ag_{18.1}$ eutectic composition which have not yet been conducted. Due to the reactivity of the system, a contactless measurement technique is preferential. Consequently, the goal of this study is the precise measurement of viscosity and surface tension of the $Al_{69.1}Cu_{12.8}Ag_{18.1}$ eutectic liquid alloy under microgravity (μg) using the oscillating-drop-method (ODM) with electromagnetic levitation (EML) [15–17] at several temperatures in the range of 900–1500 K. These are required because the enthalpy of mixing ΔH_{mix} is unknown and expected to be strongly non-zero as the mixing of the Al-Cu-Ag system is reported to be highly non-ideal [1].

The oscillating-drop-method is a common technique for contactless measurements of viscosity and surface tension of liquid freely levitated melts. By shortly squeezing of a levitated liquid droplet at different temperatures, oscillations are forced to a liquid metallic sample and the damping and its frequency are used to derive the sample's viscosity and surface tension, respectively. [18–24] For the applied ODM, μg-conditions are highly preferential compared to 1g-conditions as they allow to operate with reduced

electromagnetic positioning fields and thus reduced magnetic pressure. This allows to maintain a rather spherical shape of the specimen and to reduce the induction of turbulence to a minimum [25] and hence to enforce "clearer" oscillations in the lowest excitation mode. Nevertheless, despite being strongly mitigated in microgravity, attenuated rotation of the specimen around the z-axis still occurs, especially during heating of the specimen with maximum heater field. Figure 1 shows the plane of the levitation coil windings. The z-axis is perpendicular to that plane directed towards the top of the process chamber.

1.1 Electromagnetic levitation, TEMPUS facility, parabolic flight

Electromagnetic levitation (EML) is a contactless technique for handling and processing of electrically conducting samples inside a process chamber that is either evacuated to ultra-high-vacuum (UHV) conditions or filled with a process gas, usually Argon or Helium. Higher cooling rates generally enable to achieve high undercoolings. [26] This technique applies inhomogeneous, high-frequency (HF) electromagnetic fields, which are generated by alternating currents through suitably shaped levitation coils. These induce eddy currents inside the small (≈6.5 mm diameter) metallic specimen placed in the center of the coil. The eddy currents provide a positioning force and heat and melt the specimen due to resistive losses.

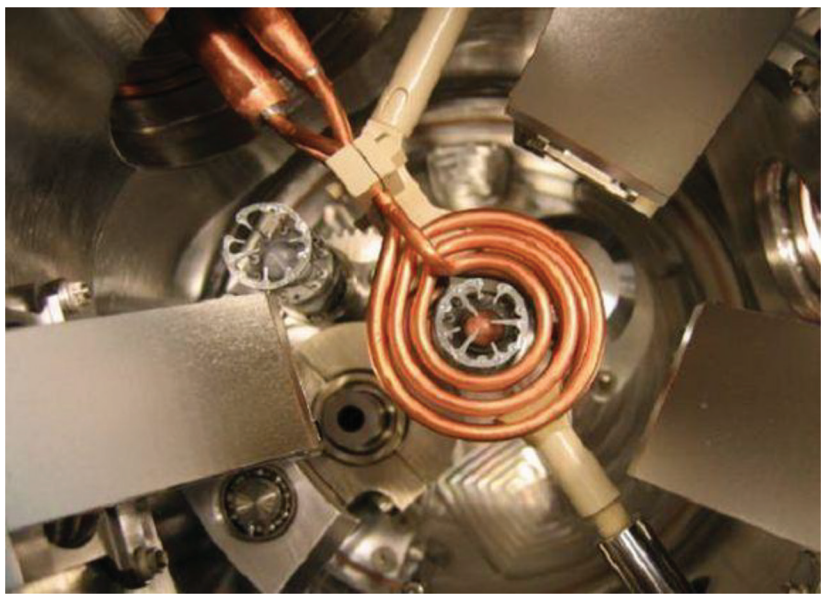

FIGURE 1
Top-view into the process chamber of TEMPUS. A sample holder prevents accidental contacts between the sample and the surrounding copper magnetic coils.

During processing, the specimen becomes part of an oscillating circuit (OC) that is operated at the resonance frequency of ≈ 380 kHz to achieve the highest power absorption. In an essentially forceless μg-environment, the lifting and positioning force is reduced by a factor of 100–1000 compared to EML under normal gravity (1g).

TEMPUS [27] is an EML-facility for levitation under microgravity that is used onboard of aircrafts during parabolic flights. Heating and positioning of the sample are performed independently by two superposed magnetic fields. A dipole field is used for heating. A typically one order of magnitude weaker quadrupole field is used for the positioning of the specimen at the center of the levitation coil. During roughly 23 seconds of one parabola, microgravity is produced due to the compensation of the gravitational forces by inertia. TEMPUS is equipped with the so called Sample Coupling Electronics (SCE) for the inductive measurement of the electrical resistivity of the levitated metallic sample [28–29]. The principle is described in detail in a work by Lohöfer *et al.* [30]. It measures the resonance frequency of the magnetic heating field. This quantity is sensitive to changes of the samples' cross section. The cross section and thus the resonance frequency are altered by the periodic sample squeezing during oscillations. It is thus a measure for the time-dependent radius of the sample and hence, for the amplitude $A\,(t)$ of the oscillation. A more detailed description is presented in ref. [31].

1.2 Formulas and Models

For the damped oscillations with a single frequency of a spherical, liquid droplet, *A(t)* can be described by the following formula,

$$A\,(t) = A_0 \cdot \sin(2\pi\nu t + \phi) \cdot \exp(-\Gamma t), \tag{1}$$

where A_0 is the amplitude, ν is the oscillation natural frequency, ϕ is the phase shift and Γ represents the damping constant. The relation between viscosity η and damping constant Γ is given by the Lamb formula [15, 20]

$$\eta = \frac{3}{20\pi}\frac{M}{r_0}\Gamma, \tag{2}$$

where r_0: radius of the spherical sample and M: sample mass. According to *Rayleigh*, in the ideal case of a spherical, force-free droplet, the relation between the observed lowest mode oscillation frequency $\nu_{l=2}$ and the surface tension γ is [32]

$$\nu_{l=2}^2 = \frac{8}{3\pi}\frac{\gamma}{M}. \tag{3}$$

The lowest mode frequency is called Rayleigh-frequency. Under normal gravity, the mode splits up into a set of 5 frequencies [33–36] due to deformations by magnetic pressure [33] and sample rotation [34] around the z-axis. Under microgravity, the weak positioning field causes only reduced deformations, and thus correction terms published by Busse *et al.* [34] and Cummings and Blackburn [33] become negligible. These are required under 1g to correct the magnetic pressure due to horizontal and vertical displacement frequencies of the sample.

The viscosity of a liquid specimen typically decays exponentially with temperature according to an Arrhenius law

$$\eta\,(T)/\mathrm{mPas} = \eta_\infty \exp\left(\frac{E_\eta}{\mathrm{R}T}\right), \tag{4}$$

where R: ideal gas constant, T: temperature in K, η_∞: viscosity for $T \to \infty$ and E_η: activation energy of viscous flow.

The Kozlov-model [14],

$$\ln(\eta) = \sum\nolimits_{i=1}^{N} c_i \ln(\eta_i) - \frac{\Delta H_{mix}}{3\mathrm{R}T}, \tag{5}$$

relates the viscosities η_i of pure elements i of an alloy with concentrations c_i to the enthalpy of mixing ΔH_{mix}, according to $\Delta H_{mix} = 0$: ideal mixing, $\Delta H_{mix} \neq 0$: non-ideal mixing. For non-ideal systems, $\eta = \eta^{id} + \eta^{E}$ holds, with "excess"-viscosity $\eta^{E} \neq 0$ and viscosity of an ideal solution $\eta^{id} > 0$ [1].

The temperature-dependence of the surface tension $\gamma\,(T)$ typically follows a linear law,

$$\gamma\,(T) = \gamma_l + \gamma_T\,(T - T_m), \tag{6}$$

where γ_l: surface tension at liquidus temperature T_m, γ_T: temperature derivative of the surface tension γ.

2 EXPERIMENTAL

The TEMPUS-facility was used onboard the Airbus A310 Zero-G in parabolic flights in the years 2015–2017 (see Table 1). The measurements were performed on similar specimen with a nominal diameter of 6.5 mm and a nominal weight of 850 mg at the eutectic composition, i.e. $Al_{69.1}Cu_{12.8}Ag_{18.1}$. The deviations of the concentration from the nominal value were below 1%. The samples were created from identical pure Al, Cu and Ag by cutting and polishing to the desired mass and alloying in arc melting (details in ref. [2]).

TABLE 1
Conducted parabolas with $Al_{68.1}Cu_{12.8}Ag_{18.1}$ with successful melting and application of heater pulses in the liquid state under µg-conditions; totally conducted parabolas: 27, success-ratio: 56%.

Year	Day	Parabola	Liquid Pulses	Specimen #
2015	2	28	2	1
2015	2	30	2	2
2016	3	21	2	3
2016	3	22	2	3
2016	3	24	2.5*	3
2016	3	26	2	4
2016	3	27	2	4
2016	3	28	2	4
2017	3	16	3	5
2017	3	17	2	5
2017	3	18	3	5
2017	3	19	3	5
2017	3	20	1	5
2017	3	22	1.5*	5
2017	3	23	1	5

*solidification occurred during damped sample oscillations.

The masses ranged from 848–866 mg and the mass loss due to evaporation was 0.5–1.2% (see Table 2). The sample temperature was measured with a pyrometer axially on the sample surface. The spectral normal emissivity $\in_{spec}$ was calibrated via the recorded temperature-time-profile (*Tt*-profile) to $\in_{spec} = 0.3$ using the known liquidus temperature, i.e. where a plateau is seen in the temperature when the melting process is completed. In a few parabolas temperatures were measured with other spectral emissivity values. Those temperatures were corrected to $\in_{spec} = 0.3$ by a formalism using the Wien-law as described in ref. [37]. During the experiment, the specimen was inside a ceramic cup sample holder to prevent direct contact to the coil. Cloverleaf-shaped cut-outs in the cup sample holders gave sight for radial high speed camera- (HSC) recordings of the sample with a frequency of 0.2–1 kHz. The oscillations were also recorded axially by an additional analog camera with 50Hz. The SCE was recording the oscillations of the magnetic heating field with a data rate of 400Hz. The oscillating-drop-method was applied via stimulation by the heater control voltage. In other words, the magnetic pressure was stimulated to squeeze and release the sample.

TABLE 2
Details of $Al_{68.1}Cu_{12.8}Ag_{18.1}$ specimen (from historical records). Al: Chempur 99.99% purity, Cu: Chempur 99.99% purity, Ag: Alfa Aesar 99.9% purity. The initial average diameter after arc melting was ~6.5 mm for all specimen with minimum values of 6.0–6.3 mm and maximum values of 6.7–6.8 mm.

Specimen #	Year	Day	Parabola	Mass [g]	Mass loss [%]
1	2015	2	26–28	0.85	1.1
2	2015	2	29–30	0.85	0.5
3	2016	3	21–25	0.856	1.2
4	2016	3	26–29	0.848	1.1
5	2017	3	16–23	0.866	0.6

Figure 2 shows the *Tt*-profile of a typical parabola that comprises the 3 phases pre-heating, heating and melting, experiment and cooling. In the pre-heating phase, starting roughly after 2/3 of the maximum altitude of the rising flank of the parabola, the gravitational force rapidly declined from hypergravity to almost zero. Due to the limited time under μg-conditions, the heating and melting phase was performed with maximum heater and positioner fields. This was done in argon-atmosphere until a pre-defined maximum temperature of ~1500 K was reached.

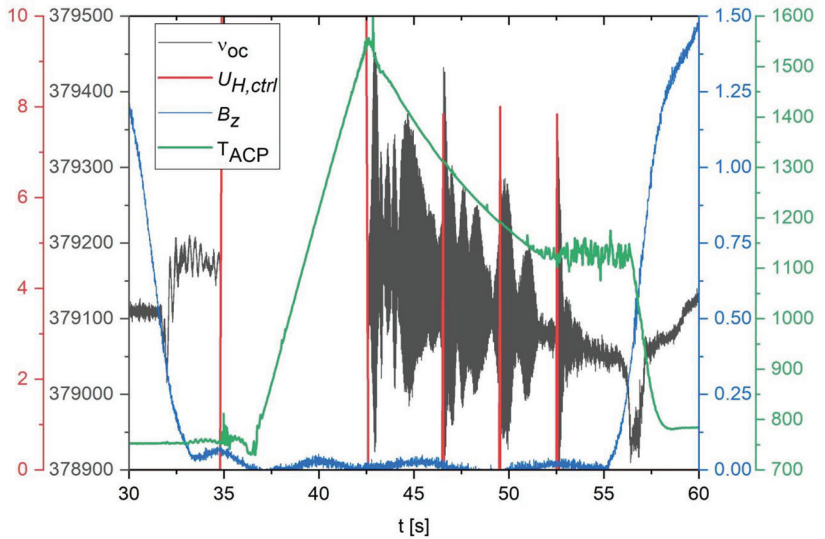

FIGURE 2
Temperature-time-profile of parabola 22 on day 3 in 2016: green: temperature in K, red: heater control voltage in V, blue: acceleration in z-direction, black: resonance frequency of the electrical heating circuit in Hz.

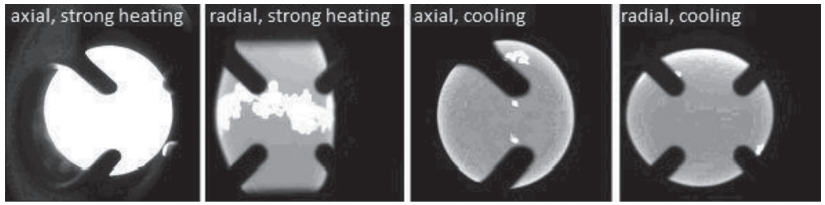

FIGURE 3
Camera views of eutectic AlCuAg at parabola 28 (μg-phase) on day 2 in 2015 (from left to right): axial (heating), radial (heating), axial (cooling), radial (cooling). During heating with maximum heater and positioner field, strong aspherical elongation occured by squeezing via magnetic pressure of the heater field. The radial view shows a dissolving "belt" of oxides on the surface. During cooling with minimum heater and reduced positioner field, an almost spherical sample oscillates "freely".

During heating, the sample was squeezed to an elongated shape (see Figure 3, "radial, strong heating") by magnetic pressure.

The transition to the experiment and cooling phase was initiated by a fast reduction of the heater field to its operational minimum and the positioner field was strongly reduced simultaneously. Cooling was supported by a He-quench, i.e. by flooding of the process chamber with He-gas in order to achieve stronger cooling rates. [26] The initial oscillation of the experiment was created by minimizing the heater field and thus releasing the squeezing of the specimen by the magnetic pressure of the dipole field. Furthermore, 3 oscillations were excited in a sequence with different delay-times in-between. This was done to achieve oscillations at different temperatures during cooling by either application of short pulses (mostly rectangle, 50–75 ms) or in some cases sine-modulations, both with the heater field. The pulses enforced "clearer" oscillations compared to the initial "no-load"-oscillation. Hence, the oscillations after pulses were measured over a narrower temperature range, because the radiative cooling rate is $\propto T^4$ and thus strongest at the maximum temperature (see Figure 2, green line). The temperature declines continuously during cooling. After each parabola, the sample was finally solidified in the double-gravity (2g) phase. In our experiment the specimen maintained an almost spherical shape during the cooling-phase (see Figure 3, "axial, cooling" and "radial, cooling") and reduced rotation-velocities around the z-axis were observed. Hence, splitting of the *Rayleigh*-mode was successfully suppressed.

3 ANALYSIS

The analysis was focused on the varying resonance frequency-data of the electrical heating circuit, which reflects the oscillation of the liquid sample. These were analyzed by Fast Fourier transformations (FFT). Hence, for each

oscillation period, the temperature was averaged over the investigated range (~2–3s).

For each parabola (see Table 1), Gaussian fits were applied to the time-averaged FFT-data after a) setting the heater control voltage to 0V, b) 1st pulse, c) 2nd pulse and d) 3rd pulse.

This was done to assess "clear" oscillations with the Rayleigh-Frequency and to allow retrieval of the surface tension γ according to eq. (3) via the natural frequency ν_0 of the peak-centre ν_0 of a Gaussian fit (see Figure 4); the $2\sigma_{\nu_0}$ of the fit parameter ν_0 was used to estimate the uncertainty of surface tension data points.

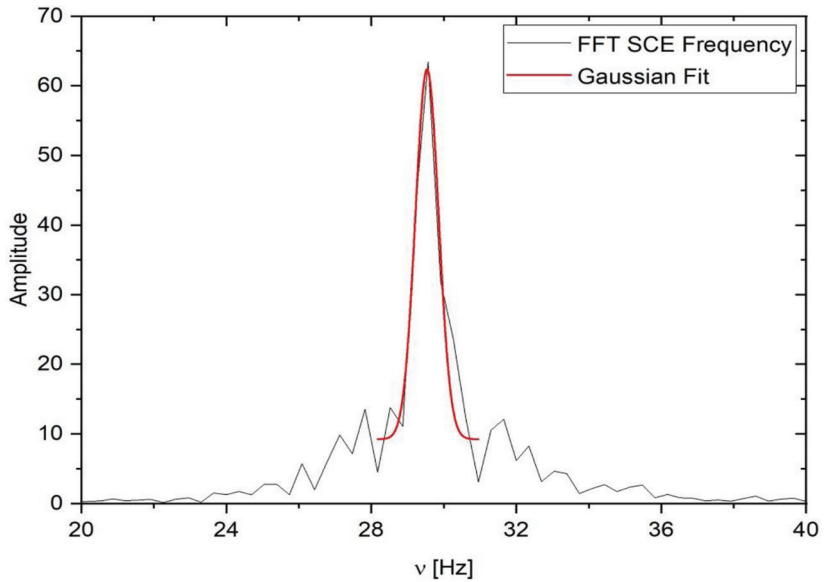

FIGURE 4
FFT of the recorded SCE-frequency after setting the heater from 10V→0V with Gaussian fit (red line) to the *Rayleigh-peak*.

3.1 Data processing

The data were processed separately for each oscillation-period. Figure 5 shows a "clear" oscillation of $Al_{69.1}Cu_{12.8}Ag_{18.1}$ and the performed analysis. The baseline was obtained by a linear fit to the recorded SCE-frequencies (see Figure 5) and then subtracted from these. The natural logarithm of the absolute of these "corrected" frequencies was plotted (see Figure 6) and fitted with a linear regression function as shown by the red curve in Figure 6. As shown by Egry *et al.* [20], the slope of the linear regression function corresponds to the damping parameter Γ of the lamb-formula.

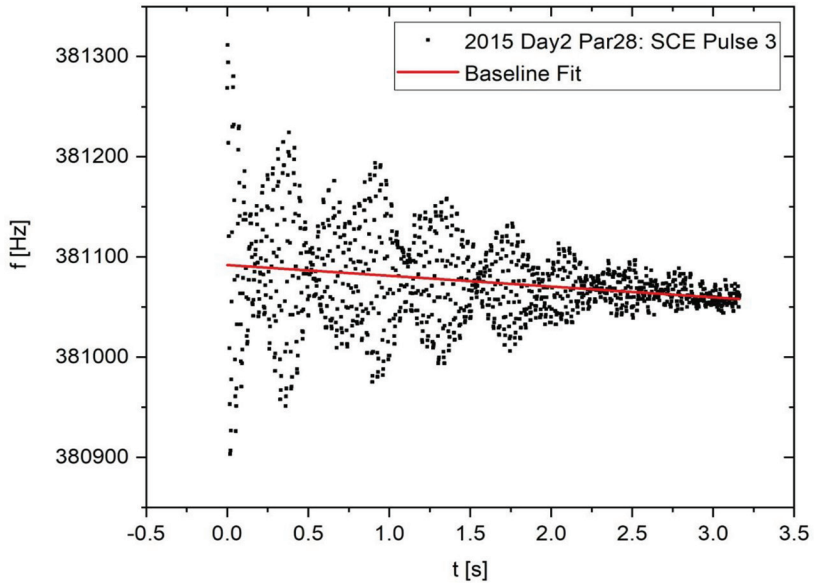

FIGURE 5
Parabola 28 on day 2 in 2015: linear baseline-fit to the SCE data after the 3rd pulse.

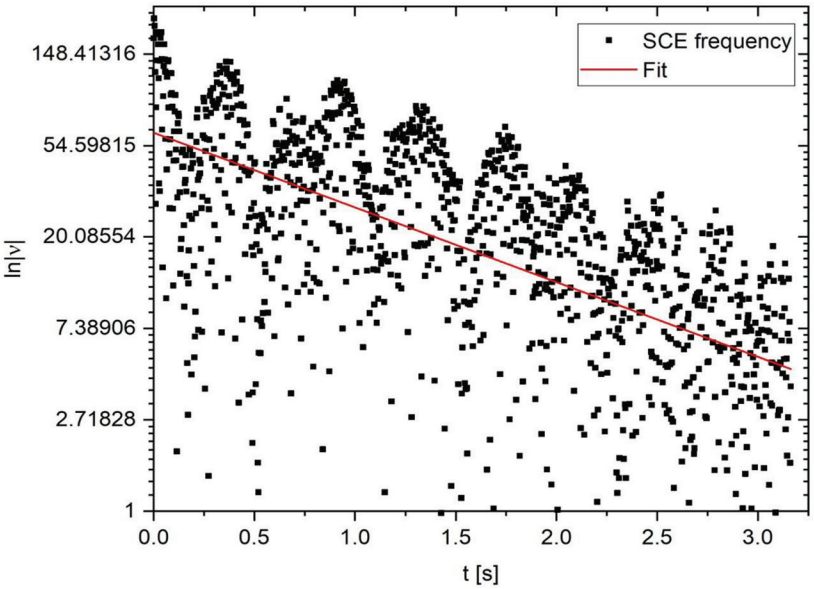

FIGURE 6
Parabola 28 on day 2 in 2015: linear fit to the natural logarithm of the absolute of the baseline-subtracted SCE-data.

The viscosity was finally calculated from the fit parameter Γ according to eq. (2) and the uncertainty was calculated accordingly from the $2\sigma_\Gamma$ of the fit parameter Γ.

One important question was how the number of data points affects the soundness of the used algorithm. A very simple test was the application of the algorithm to a generated signal of ideal, unperturbed single-frequency oscillations as given by eq. (1). In such a simplified special case, 1000 data points are sufficient to keep the deviation of the resulting Γ parameter compared to the inserted Γ parameter below 2.7%. This was regarded as acceptable and consequently only oscillation periods with more than 1000 recorded data points were analyzed.

4 RESULTS

Viscosity and surface tension of the ternary eutectic $Al_{69.1}Cu_{12.8}Ag_{18.1}$ were derived from the measured resonance frequency of the oscillating circuit via eqs. (2) and (3). The variations of this frequency were $\Delta\nu_{oc} \leq 550$ Hz and thus with a relative signal strength of $\Delta\nu_{oc}/\nu_{oc} \leq 1.5 \cdot 10^{-3}$, see Figure 2, black line.

4.1 Viscosity

From the obtained viscosity values those with the highest significance of the Γ-parameter of the fit (t-value) and highest significance of regression (corr. R^2, Pearson R, F-value of analysis of variance) were selected. The plausibility of the selection was confirmed by evaluation of the Fast-Fourier-Transform spectra and observation of oscillations via the radial high-speed-camera videos. Oscillation periods comprised between 1044 and 1551 data points each.

The results are shown in Figure 7 and Table 3. The measured temperatures decreased exponentially with rising temperature from 10.21 mPas at 1016 K to 4.41 mPas at 1416 K. The temperature uncertainty was ± 67 K at 1416 K and ± 13 K at 1016 K. It was basically proportional to the temperature itself for similar amount of oscillation data points due to the highly non-linear temperature-dependence of the radiative cooling. The uncertainty of the viscosity values was randomly ranging from ± 0.29 mPas at 1416 K to ± 0.52 mPas at 1225 K with a mean uncertainty of ± 0.44 mPas.

4.2 Surface tension

Surface tension data were selected from 11 successful parabolas for pronounced Rayleigh-peaks in the FFT spectrum, i.e. in cases where the centre of the gaussian fit was corresponding to the visible peak maximum of the FFT spectrum (as in Figure 4). Data was retrieved for temperatures between 914.8 K and 1485.4 K and slightly decreasing with increasing temperatures.

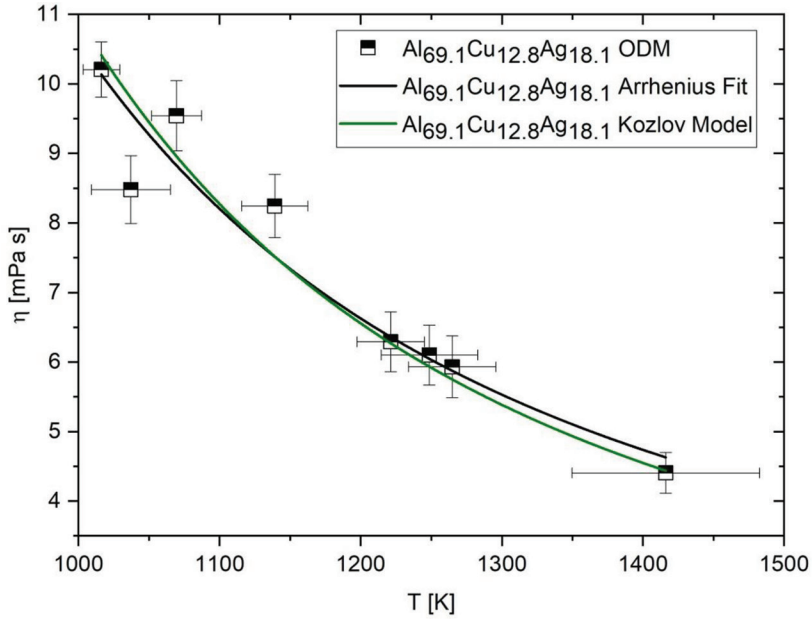

FIGURE 7
Viscosity η of $Al_{69.1}Cu_{12.8}Ag_{18.1}$ Vs. temperature T. An Arrhenius-fit $\eta(T) = 0.632 \cdot \exp(23440/RT)$ to the data is shown as well as a fit with the Kozlov-model, eq. (7), using single-element viscosity data from Brillo *et al*. [11]. All data points are in the liquid state ($T_l = 774$ K).

TABLE 3
Analyzed data of Figure 6: fit parameter Γ with std.-deviation σ_Γ and corresponding cor. R^2, Pearson R, calculated viscosity η with std.-deviation σ_η, measured temperature T with std. deviation σ_T; pulse = 0,1,2,3: oscillation periods; 0 = "heater off".

Year	Day	Par	Pulse	Γ	σ_Γ	t_Γ	Cor. R^2	Pearson-R	F	η	σ_η	T	σ_T
										[*m*Pas]	[*m*Pas]	[K]	[K]
2015	2	28	3	–0.82	0.03	–25.6	0.34	–0.58	657	10.21	0.40	1016	13
2015	2	30	1	–0.68	0.04	–17.4	0.21	–0.45	303	8.48	0.49	1037	28
2016	3	22	1	–0.49	0.03	–14.2	0.15	–0.38	201	6.10	0.43	1249	34
2016	3	24	0	–0.35	0.02	–15.0	0.14	–0.36	226	4.41	0.29	1416	67
2016	3	26	2	–0.50	0.03	–14.6	0.16	–0.40	215	6.29	0.43	1221	24
2017	3	19	1	–0.66	0.04	–18.0	0.22	–0.47	324	8.24	0.46	1139	23
2017	3	19	2	–0.76	0.04	–18.9	0.24	–0.49	357	9.54	0.51	1069	18
2017	3	20	1	–0.47	0.04	–13.3	0.13	–0.37	178	5.93	0.44	1265	31

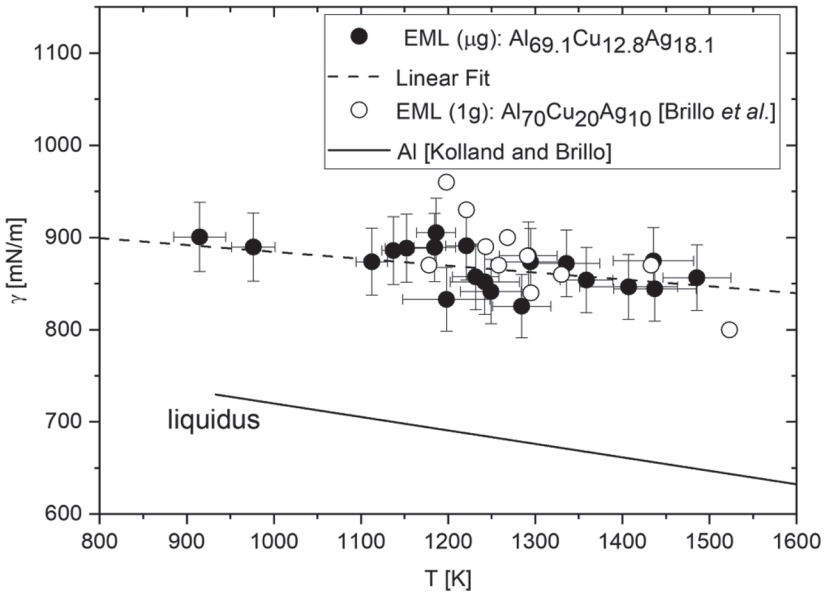

FIGURE 8
Surface tension γ of $Al_{69.1}Cu_{12.8}Ag_{18.1}$ vs. temperature T with linear fit: eq. (7); 1g-data from Brillo et al. for $Al_{70}Cu_{20}Ag_{10}$ is taken from Figure 3 in [10]. A linear fit for pure Al is shown with data from Table A.3. in ref. [1].

Most data points were obtained for temperatures between 1100 K and 1300 K. The maximum scatter of the data from measurements at almost the same temperature, was observed at approx. 1192 K. It was $\Delta\gamma(T' \approx 1192\ \mathrm{K}) = 905.260\frac{\mathrm{mN}}{\mathrm{m}}(1186.2\ \mathrm{K}) - 832.879\frac{\mathrm{mN}}{\mathrm{m}}(1198\ \mathrm{K}) = 72.381\frac{\mathrm{mN}}{\mathrm{m}}$, which is equivalent to a maximum relative scatter of $\frac{\Delta\gamma\,(T)}{\gamma'\,(T')} = \frac{72.381\ \mathrm{mN/m}}{869.07\ \mathrm{mN/m}\ (1192.1\ \mathrm{K})} = 0.083$. The uncertainty of the determined surface tension values was governed by the frequency-resolution of the SCE (0.37 Hz, ~1.3% of the Rayleigh frequency), the mass loss (evaporation rate), changes of the surface-composition of the specimen (transport dynamics), and the uncertainty σ_{ν_0} of the fit parameter ν_0 of the peak centre in the FFT spectrum. The evaporation rate and the transport dynamics were not measured or simulated in the frame of this work. Thus, a conservative relative uncertainty of $\pm 4.15\%$ was assumed for each data point, being half of the observed maximum relative scatter.

5 DISCUSSION

Even though dissolved oxygen and sulfur were observed (see Figure 3, "oxide-belt") but not quantified in the frame of this work, the samples were

considered to be fairly clean. This was indicated by comparably small fluctuations in the measured temperature-time-profiles during heating and cooling. During cooling, a sudden scatter in the temperature-measurements coincided with reappearance of dissolvants at the surface of the specimen. This became visible at temperatures below 1130 K (see Figure 2) and may have affected 3 surface tension data points that were obtained at lower temperatures. The evaporated mass loss of the used specimen was 0.5%–1.2% (see Table 2).

5.1 Viscosity

An Arrhenius-fit as given by eq. 4 was applied to the viscosity data of $Al_{69.1}Cu_{12.8}Ag_{18.1}$ (see Figure 7), yielding $\eta_\infty = (0.632 \pm 0.160)$ mPas and activation energy for viscous flow $E_\eta = (2.344 \pm 0.233) \cdot 10^4$ J/mol. The fit was highly significant. It had a corrected R^2 value of 0.939. This expression is the central result of this work.

The expression of the Kozlov-model as given by eq. 5 was used with single-element data for Al, Cu and Ag from Arrhenius fits published by Brillo *et al.* in ref [11] (E_i and $\eta_{\infty,i}$: see Table 5). The Kozlov model expression was fit to the viscosity data with a corrected R^2 value of 0.992. It yielded a strongly negative enthalpy of mixing $\Delta H_{mix} = -(18.576 \pm 0.018)$ kJ/mol. This implies a positive "excess"-viscosity $\eta^E \gg 0$. Furthermore, the curvature was comparable to the one of the Arrhenius fit. Hence, we can conclude that the temperature sensitivity was comparable to an ideal solution. Our findings for the mixing behavior of eutectic $Al_{69.1}Cu_{12.8}Ag_{18.1}$ are in agreement with findings by Brillo who investigated the general mixing behavior of ternary Al-Cu-Ag systems and concluded those to be strongly "non-ideal", with negative enthalpy of mixing $\Delta H_{mix} < 0$ and positive "excess"-viscosity $\eta^E > 0$ [1].

5.2 Surface tension

The surface tension of the eutectic $Al_{69.1}Cu_{12.8}Ag_{18.1}$ composition was in the same order as data published by Brillo *et al.* [10] for $Al_{70}Cu_{20}Ag_{10}$ (EML-ODM, normal gravity), especially for temperatures between 1150 K and 1500 K. A linear fit was applied to the data of the eutectic liquid alloy, according to eq. 6 (see Figure 8). The surface tension at liquidus-temperature was $\gamma_l = (0.9013 \pm 0.02625)$ Nm^{-1} and the temperature derivative was $\gamma_T = -(0.7462 \pm 0.2675) \cdot 10^{-4}$ $Nm^{-1}K^{-1}$. The latter parameter had a huge relative uncertainty of $\pm 35.8\%$. The eutectic composition was less sensitive to temperature (γ_T-value) than $Al_{70}Cu_{20}Ag_{10}$. This is likely due to the higher Al- and lower Cu-content of the eutectic liquid alloy. The linear fit to our data was not significant and had a low corrected R^2 value of 0.25328. Hence, linearity in T had to be assumed and could not be proven by our measurements. This was most probably mainly due to the comparably small temperature sensitivity itself (γ_T-value), because in such a case the weak linear behavior is easily

TABLE 4
Analyzed FFT-data with ν_0: peak-centre of gaussian fit with std.-deviation σ_{ν_0} and corresponding cor. R^2, calculated surface tension γ with std.-deviation σ_γ, measured temperature T with std. deviation σ_T; pulse = 0,1,2,3: oscillation periods; 0 = "heater off".

Year	Day	Par.	Pulse	ν_0	σ_{ν_0}	cor. R^2	γ	σ_γ	T	σ_T
				[Hz]	[Hz]		[mN/m]	[mN/m]	[K]	[K]
2015	2	28	1	28.840	0.042	0.912	832.879	0.0016	1198.0	38.1
2015	2	30	2	29.807	0.080	0.744	889.676	0.0057	976.4	16.7
2015	2	30	3	29.990	0.039	0.765	900.619	0.0013	914.8	16.0
2016	3	21	1	29.167	0.042	0.780	851.871	0.0016	1242.0	39.7
2016	3	21	3	29.742	0.071	0.939	885.807	0.0045	1137.0	13.2
2016	3	22	1	28.986	0.080	0.772	841.349	0.0057	1248.9	34.8
2016	3	24	0	29.202	0.140	0.641	853.950	0.0173	1358.7	30.1
2016	3	24	3	29.539	0.156	0.748	873.750	0.0215	1112.3	18.0
2016	3	26	0	29.245	0.031	0.974	856.445	0.0008	1485.4	39.0
2016	3	26	1	29.510	0.067	0.759	872.026	0.0040	1335.6	38.4
2016	3	26	2	29.829	0.075	0.806	890.991	0.0050	1221.0	23.8
2016	3	27	1	29.650	0.062	0.653	880.351	0.0034	1292.0	33.3
2016	3	27	2	30.067	0.022	0.971	905.260	0.0004	1186.2	22.2
2016	3	28	0	29.074	0.041	0.881	846.467	0.0016	1407.1	56.2
2016	3	28	2	29.787	0.081	0.728	888.491	0.0058	1152.3	24.7
2017	3	17	0	29.038	0.002	0.999	844.362	5.4e-6	1437.1	47.5
2017	3	17	1	28.714	0.009	0.997	825.609	7.16e-5	1284.3	33.5
2017	3	17	2	29.802	0.024	0.934	889.364	0.0005	1184.5	23.8
2017	3	19	0	29.260	0.055	0.853	857.314	0.0027	1231.4	26.5
2017	3	23	0	29.556	0.031	0.872	874.750	0.0009	1435.6	46.2
2017	3	23	1	29.538	0.045	0.884	873.673	0.0018	1294.4	37.5

TABLE 5
Single element viscosity data from Arrhenius Fits published by Brillo *et al.* in ref. [11] for pure Al, Cu and Ag.

	Al	Cu	Ag
E [10^4 J/mole]	1.31	2.29	2.03
η_∞[mPa s]	0.257	0.597	0.589

superimposed by the observed scatter of data at very similar temperatures. The scatter itself was in the usual order of some percent. This was revealed by comparison with data reported for $Al_{70}Cu_{20}Ag_{10}$ by Brillo *et al.* (Figure 8).

6 CONCLUSIONS

The goal of this work was the measurement of viscosity and surface tension of an eutectic $Al_{69.1}Cu_{12.8}Ag_{18.1}$ liquid alloy at various temperatures by application of the oscillating-drop-method under microgravity conditions. This implied the derivation of a parametric representation of the temperature-dependence, which was achieved by an Arrhenius-fit to the viscosity data (eq. 4) and a typical linear fit to the surface tension data (eq.6). Furthermore, the Kozlov-model (eq. 5) was applied to determine the enthalpy of mixing ΔH_{mix} from the measurements.

The measurements were performed under microgravity during 3 parabolic flight campaigns in the years 2015, 2016 and 2017 onboard the Airbus A310 Zero-G. The electromagnetic levitation facility TEMPUS was used for the containerless processing of the material to avoid reactions of the specimen with a crucible. In total, 27 parabolas were flown for collection of sufficiently clear data for the performed analysis. 15 out of those were evaluated successfully at various temperatures. 8 out of 31 oscillations in the liquid state resulted in valid data points for the viscosity of the specimen and 21 out of 31 excited oscillations were evaluated for surface tension analysis.

From the resulting frequency spectra only those which showed one clear Rayleigh-peak around ~30 Hz were considered for further evaluation. In this case, which only occurs under low gravity conditions, the surface tension was calculated with the Rayleigh-formula and a linear fit to the data yielded $\gamma_l = (0.9013 \pm 0.02625)\ \mathrm{Nm}^{-1}$ and $\gamma_T = -(0.7462 \pm 0.2675) \cdot 10^{-4}\ \mathrm{Nm}^{-1}\mathrm{K}^{-1}$.

For viscosity analysis, goals were the fit of an Arrhenius law for the temperature dependence and usage of the Kozlov model for assessment of the enthalpy of mixing. A linear baseline fit-function was subtracted separately for each oscillation-period. After baseline-subtraction, a linear fit was applied to the natural logarithm of the absolute of the baseline-subtracted frequency data. The slope was equivalent to the damping constant Γ as in eq. (1). The soundness of this method for viscosity-analysis was shown by Egry *et al.* [20]. Finally, the most reliable data was selected and an Arrhenius function was fit to the data with $\eta_\infty = (0.632 \pm 0.160)$ mPas and activation energy for viscous flow of $E_\eta = (23.44 \pm 2.33)$ kJ/mol. The measured viscosities showed a high correlation to the Arrhenius-fit function, expressed by a corrected $R^2 = 0.939$. A fit of the Kozlov-model to the viscosity data yielded a value for the enthalpy of mixing of $\Delta H_{mix} = -(18.576 \pm 0.018)$ kJ/mol. Hence, the non-ideal mixing behavior that was reported for different AlCuAg-systems by Brillo [1] was confirmed for the eutectic liquid alloy.

ACKNOWLEDGEMENTS

We would like to thank the members of the TEMPUS team for supporting the experiment planning and performing operations of the TEMPUS facility. We further thank the German Space Agency in Bonn and the European Space Agency for financially enabling us to participate in the parabolic flight campaigns in the years 2015, 2016 and 2017. We further thank J. Brillo and G. Lohöfer for their support.

REFERENCES

[1] Brillo, J. *Thermophysical Properties of Multicomponent Liquid Alloys*. Berlin, Boston: De Gruyter Oldenbourg; 2016. https://doi.org/10.1515/9783110468991
[2] Engelhardt, M. *PhD thesis*. Technische Hochschule Aachen, Aachen; 2014
[3] Brillo, J., Arato, E., Giuranno, D., Kobatake, H., Maran, C., Novakovic, R., Ricci, E., Rosello, D. *High Temp. – High Press.* **47** (2018), 417–441
[4] Griesche, A., Macht, M. P., Frohberg, G. *Journal of Non-Crystalline Solids* **353** (2007), 3305–3309. https://doi.org/10.1016/j.jnoncrysol.2007.05.076
[5] Zhang, B., Griesche, A., Meyer, A. *Phys. Rev. Lett.* **104** (2010), 035902. https://doi.org/10.1103/PhysRevLett.104.035902
[6] Gupta, P., Doraiswami, R., Tumala, R. *Electron. Compon. Technol.* **1** (2004), 68. https://doi.org/10.1109/ECTC.2004.1319317
[7] Hahn, C., Hans, M., Hein, C., Mancinelli, R.L., Wirth, R., Rettberg, P., Hellweg, C.E., Moeller, R. *Astrobiology* **17** (2017), 12*,* 1–9. https://doi.org/10.1089/ast.2016.1620
[8] Zimmermann, G., Hecht, U., Mathes, M., Mathiesen, R. H. *International Journal of Materials Research* **101** (2010), 1484–1488. https://doi.org/10.3139/146.110435
[9] Witusiewicz, V.T., Hecht, U., Fries, S.G., Rex, S. *Journal of Alloys and Compounds* **387** (2005), Issues 1–2, 217–227. https://doi.org/10.1016/j.jallcom.2004.06.078
[10] Brillo, J., Plevachuk, Y., Egry, I. *J. Mater. Sci.* **45** (2010), 5150–5157. https://doi.org/10.1007/s10853-010-4512-6
[11] Brillo, J., Brooks, R., Egry, I., Quested, P. *High Temp. – High Press.* **37** (2008), 4, 371–381
[12] Ferreira, I.L., de Castro, J.A., Garcia, A. *Continuum Mech. Thermodyn.* **31** (2019), 1369–1385. https://doi.org/10.1007/s00161-019-00753-7
[13] Dinsdale, A. T., Quested, P. N. *Journal of Materials Science* **39** (2004), 7221–7228
[14] Kozlov, L.Y., Romanov, L.M., Petrov, N.N. *Vuzov Izv. Chernaya Metall.* **3** (1983), 7
[15] Okress, E. C., Wroughton, D. M. *J. Appl. Phys.* **23** (1952), 545–552. https://doi.org/10.1063/1.1702249
[16] Bedford, B. D., Peer, L. H. B., Tonks, L. *General Electric Review* **42** (1939), 6, 246–247
[17] Lohöfer, G. *J. Appl. Math.* **49** (1989), 567–581
[18] Egry, I., Lohöfer, G., Jacobs , G. *Phys. Rev. Lett.* **75** (1995), 4043. https://doi.org/10.1103/PhysRevLett.75.4043
[19] Egry, I., Diefenbach, A., Dreier, W., Piller, J. *International journal of Thermophysics* **22** (2001), 2, 569–578. https://doi.org/10.1023/A:1010753805462
[20] Egry, I., Giffard, H., Schneider, S. *Measurement Science and Technology* **16** (2005), 426–431. https://doi.org/10.1088/0957-0233/16/2/013
[21] Wunderlich, R. *High Temperature Materials and Processes* **27** (2008), 401–412. https://doi.org/10.1515/HTMP.2008.27.6.401
[22] Mohr, M., Wunderlich, R.K., Zweiacker, K., Prades-Rödel, S., Sauget, R., Blatter, A., *et al. npj Microgravity* **5** (2019)**,** 4, 1–8. https://doi.org/10.1038/s41526-019-0065-4
[23] Higuchi, K., Fecht, H.-J., Wunderlich, R. *Adv. Eng. Mater.* **9** (2007), 349–354. https://doi.org/10.1002/adem.200600277
[24] Wunderlich, R. K., Fecht, H.-J., Lohöfer, G. *Metall. Mater. Trans. B* **48B** (2017), 237

[25] Xiao, X., Lee, J., Hyers, R.W., Matson, D. M. *npj Microgravity* **5** (2019)**,** 7, 1–7. https://doi.org/10.1038/s41526-019-0067-2
[26] Lohöfer, G., Schneider, S. *High Temp. – High Press.* **44** (2015), 6
[27] Lohöfer, G., Neuhaus, P., Egry, I *High Temp. – High Press.* **23** (1991), 333–342
[28] Lohöfer, G. *Review of Scientific Instruments* **89** (2018), 12, 124709. https://doi.org/10.1063/1.5065482
[29] Lohöfer, G. *Meas. Sci. Technol.* **16** (2005), 417. https://doi.org/10.1063/1.5065482
[30] Lohöfer, G., Pottlacher, G. *High Temp. – High Press.* **40** (2011), 237
[31] Kobatake, H., Brillo, J. *High Temp. – High Press.* **47** (2018), 465–477
[32] Rayleigh, L. *Proc. R. Soc.* **29** (1879), 71–97
[33] Cummings, D., Blackburn, D. *J. Fluid. Mech.* **224** (1991), 395–416
[34] Busse, F. H. *J. Fluid. Mech.* **142** (1984), 1–8. https://doi.org/10.1017/S0022112084000963
[35] Chandrasekhar, S. *Proc. Math. Soc.* **9** (1959), 141–149. https://doi.org/10.1112/plms/s3-9.1.141
[36] Reid, W. H. *Appl. Math.* **18** (1960), 86–89
[37] Krishnan, S., Hansen, G. P., Hauge, R. H., Margrave, J. L. *High. Temp. Sci.* **29** (1990), 17.